Preparation and Properties of $Ti_{0.997}V_{0.003}O_2$ Photocatalyst Supported on Indonesian Natural Zeolite Using Sonochemical Method

IOP Conf. Series: Materials Science and Engineering **622** (2019) 012006 doi:10.1088/1757-899X/622/1/012006

Preparation and Properties of $Ti_{0.997}V_{0.003}O_2$ Photocatalyst Supported on Indonesian Natural Zeolite Using Sonochemical Method

Nur Aini[1*], Siti Nur Chasanah[1], Susi Nur Khalifah[1], Aminatus Arifah[1], Anton Prasetyo[1], Veinardi Suendo[2,3]

[1] Department of Chemistry, Faculty of Science and Technology, Universitas Islam Negeri Maulana Malik Ibrahim Malang, Jl. Gajayana 50, Malang 65144, Indonesia
[2] Inorganic and Physical Chemistry Research Group, Faculty Mathematics and Natural Sciences, Institut Teknologi Bandung, Jl. Ganesha 10, Bandung 40132, Indonesia
[3] Research Center for Nanosciences and Nanotechnology, Institut Teknologi Bandung, Jl. Ganesha 10,Bandung 40132, Indonesia

*Corresponding author: nuraini@kim.uin-malang.ac.id / nuraini.kkfamaliki@gmail.com

Abstract. Anatase phase of Titanium dioxide (TiO_2) is a wide bandgap semiconductor which is active as photocatalyst material under ultraviolet light irradiation. Vanadium dopant has reported to enhance its photocatalytic properties toward visible light irradiation. However, vanadium doped TiO_2 has several limitations for further practical application such as its low surface area and difficult in recycling due to its superfine particle. Supporting this material into porous and large surface material like zeolite material supposed to improve its photocatalytic properties. In this research, vanadium doped TiO_2 ($Ti_{0.997}V_{0.003}O_2$) photocatalyst was supported on Indonesian natural Zeolite using sonochemical method to study the structural and optical properties of supported photocatalyst. $Ti_{0.997}V_{0.003}O_2$ was loaded into zeolite at various concentration ranging from 10 to 30 % w/w. The X-Ray Diffraction (XRD) data showed that $Ti_{0.997}V_{0.003}O_2$/Zeolite at various concentrations have characteristic of anatase, rutile and mordenite phase structure. Infrared spectra showed the typical vibrational mode of TiO_2 and mordenite phase. The sharp peak at 1370 cm-1 which is attributed to the lattice vibration of TiO_2 became weaker due to vanadium dopant. The Raman spectra showed that the anatase vibration mode position shifted to higher wavenumber caused by the interaction between $Ti_{0.997}V_{0.003}O_2$ and zeolite. Diffuse Reflectance Spectroscopy (DRS) data revealed that 15% of $Ti_{0.997}V_{0.003}O_2$ on Zeolite has the highest visible light absorption and the lowest band gap energy (2.77 eV or 447 nm) in comparison to the others composition.

Keywords: TiO_2, photocatalyst, zeolite, vanadium, anatase

1. Introduction

Titanium dioxide (TiO_2) is one of the most investigated semiconductor for photocatalytic process. Anatase phase of TiO_2 has widely applied as heterogenous photocatalyst material because of its high thermal stability, redox ability, photocatalytic activity and photocatalytic efficiency. However, photocatalytic properties of anatase phase only occur at ultraviolet light since it has a wide bandgap energy (3.2 eV). Modification to its bandgap energy by inserting metal dopant reported to shift and enhance its optical absorption toward visible light irradiation. Metal dopant provides a new state energy level between valence band and conduction band resulted in extended light absorption in visible range. Metal dopant also serve as acceptor or donor level in wide band TiO_2 so it can reduce the recombination process of electron-hole during photocatalytic activity. Among various metal dopant, vanadium dopant at low concentration has reported to produce a wider absorption in visible region [1-3] and lowering the band gap energy of anatase phase [4] therefore it become potential material to be applied as visible light photocatalyst. Vanadium dopant also reported to suppress the recombination rate of generated electron-hole [5] so it can increase the redox reaction in photocatalytic process.

However, earlier studies were reported that undoped TiO_2 itself has another limitations for practical application such as low surface area [6], low adsorption capacity [7], difficulty in recycling and agglomeration tendency of superfine particle TiO_2 [8]. An approach to overcome this limitation is supporting this material into a porous and large surface area material to improve its photocatalytic efficiency. Among various support, zeolites are the most potential candidate since this materials have high chemical stability, large surface area, various types of unique structure, and various type of pore and channel. Supported photocatalyst on zeolite reported has higher photocatalytic activity than SiO2 support [9]. TiO_2 has been successfully supported on various type of zeolite such as Zeolite Y [10] and Clinoptilolite type of zeolite [11]. Doped TiO_2 photocatalyst which is supported on zeolites were also reported for La and Ce doped TiO_2/ZSM-5 [12], Fe doped TiO_2/Zeolite Y [13], Cr doped TiO_2/ZeUI [9], and Pt doped TiO_2/Zeolite [14]. All those supported photocatalyst confirmed to have higher photocatalytic activity and efficiency [8-13], have higher degradation rate [10], and produce excellent reusability [11] than the unsupported photocatalyst. Based on those enhanced properties, Vanadium doped TiO_2 has potential to be modified by supporting this material into zeolite.

In our previous research [15], 0.3% of vanadium was successfully doped into TiO_2 ($Ti_{0.997}V_{0.003}O_2$) by sonochemical method at 500˚C. $Ti_{0.997}V_{0.003}O_2$ has enhanced visible absorption. Immobilization this photocatalyst into porous material such Indonesian natural zeolite has become our concern for further investigation. Supporting $Ti_{0.997}V_{0.003}O_2$ into zeolite supposed to has synergetic effect between adsorption capacity from zeolite material, photocatalytic ability of TiO_2 and visible light driven absorption of vanadium dopant. Indonesian natural zeolite has chosen in this research because of its unique structure, low cost and abundant resources in Indonesia [16]. Sonochemical method was employed on loading process to take the advantages of ultrasound radiation and its cavitation phenomenon. Sonochemical method provide efficient supporting process because its relatively shorter reaction time than conventional impregnation or sol gel method. Ultrasound irradiation in sonochemical method generate acoustic cavitation [17] which is subsequently provide an hot spot reaction with high temperature and pressure in very short time. This cavitation phenomenon supposed to improve the immobilization of vanadium doped TiO_2 into zeolite's pore and channel. This research focused to study the properties of $Ti_{0.997}V_{0.003}O_2$/zeolite at various concentration (w/w ratio) between $Ti_{0.997}V_{0.003}O_2$ and zeolite to learn the structural properties, interaction and absorption characteristic.

2. Materials and methods

2.1. Materials

Titanium isopropoxide (TTIP, Sigma Aldrich), Vanadium acetylacetonate (V(acac)3, Sigma Aldrich), Isopropanol (C3H8O, E Merck), Indonesian Natural Zeolite, Hydrochloric Acid (HCl, E Merck).

2.2. Preparion of Natural zeolite

Indonesian natural zeolite (INZ) were treated before used as supporting material. INZ was activated by immersing this material in HCl 6M for 24h. Immersed zeolite then filtered, washed and neutralized with aquadest until pH 7 then calcined at 550 ^{o}C for 4h.

2.3. Preparion of $Ti_{0.997}V_{0.003}O_2$/Zeolite

Vanadium doped TiO_2 ($Ti_{0.997}V_{0.003}O_2$) was supported on activated zeolite at various concentration between $Ti_{0.997}V_{0.003}O_2$ over zeolite at w/w ratio. Prepared material were 10/90, 15/85, 20/80, 25/75, and 30/70 (% w/w). Sonochemical method was employed to immobilized titanium and vanadium precursor on zeolite. Preparation proceed by in situ reaction under ultrasound wave irradiation which generated from ultrasonic bath reactor (40 kHz, 100W).

First, Titanium isopropoxide was dissolved in 60 mL isopropanol and sonicated for 15 minutes to achieve homogenous titanium solution. Second, 0.3% of vanadium acetylacetonate ($V(acac)_3$ sigma aldrich) which previously dissolved in 10mL isopropanol added into titanium solution and sonicated for 15 minutes to obtain homogenous mixture of titanium-vanadium solution. Third, activated zeolite (dispersed in 50mL aquades) added into titanium-vanadium solution at stoiciometric amount of w/w ratio. Low intensity of ultrasonic radiation subsequently introduced into solution used ultrasonic bath reactor. The homogenous mixture in erlenmeyer flask transferred into ultrasonic bath (in water medium) then irradiated with low frequency ultrasound wave for 2h. The obtained precipitate was subsequently aged for 48h, then filtered, dried at 110˚C (2h), and calcined at 550˚C (4h). Undoped TiO_2 and $Ti_{0.997}V_{0.003}O_2$ were also prepared using the same method for further comparison between undoped, doped and supported photocatalyst at various composition. Comparison studies needed to understand the contribution of different component in this material due to its relatively complex system caused by in situ preparation.

2.4. Characterization of $Ti_{0.997}V_{0.003}O_2$/Zeolite

The structure of undoped TiO_2, $Ti_{0.997}V_{0.003}O_2$ and supported photocatalyst at w/w ratio were characterized by Powder X-Ray Diffraction (XRD). XRD data measured by XPert MPD Diffractometer using Cu-Kα radiation at 2θ 5-90˚. The XRD data compared with ICSD (Inorganic Crystal Structure Database) standard for various phase of TiO_2 and IZA structure for zeolite phase. Furthermore, XRD data was analyzed by Le Bail Refinement method using Rietica program in order to obtain the crystallographic data. The typical vibrational mode of structure studied with Infrared Spectroscopy (IR) of FT 1000 Varian instrument at 450-4000 cm^{-1}. Vibrational mode of local structure collected with by Bruker senterra of Raman spectrometer at wavenumber range 30-1560 cm-1 and resolution ~3-5 cm-1 using green laser (532 nm) as the source of excitation. The reflectance properties were measured by UV-Vis Diffuse Reflectance spectroscopy (DRS) Shimadzu UV-2450 at wavelength range 100-900nm. Collected reflectance data (R) converted to Kubelka-Munk function ($F(R)=(1-R^2/2R$). The band gap energy determined from threshold energy ($h\nu_0$) between $(F(R)h\nu)^{½}$ versus photon energy ($h\nu$) graph.

3. Results and discussion

3.1. Structural Properties

XRD Pattern of Indonesian Natural Zeolite has agreement with structural characteristic of mordenite topology (MOR Zeolite). Refinement process accomplished by using mordenite standard from IZA Structure. Refinement result revealed that mordenite's zeolite cystallized in orthorombic lattice with *Ccmc* space group (Figure 1). Unit cell parameter of modernite were a=18.1100 Å, b=20.5300 Å, c=7.5279 Å, α=90˚, asymmetric unit (Z) =1 and cell volume (V) = 2798.8979 $Å^3$. XRD pattern of $Ti_{0.997}V_{0.003}O_2$ on zeolite at various w/w ratio presented in Figure 2 along with undoped TiO_2 and vanadium doped TiO_2 ($Ti_{0.997}V_{0.003}O_2$). Undoped TiO_2 shown characteristic structure of anatase phase of TiO_2. Several peaks related to rutile phase of TiO_2 was detected while vanadium dopant introduced

in TiO_2 lattice. The rutile phase formation may led by preparing condition including the nature of vanadium dopant, sonochemical method and temperature employed.

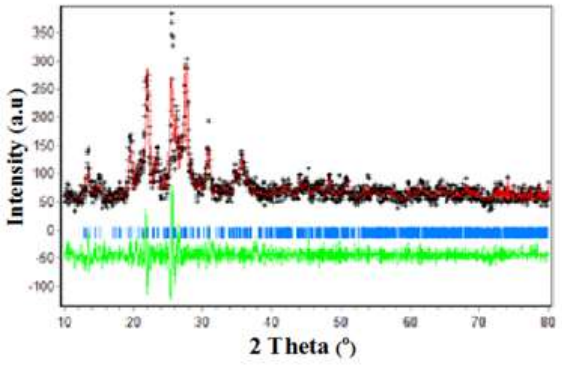

Figure 1. Plot of Le Bail refinement of mordenite zeolite.

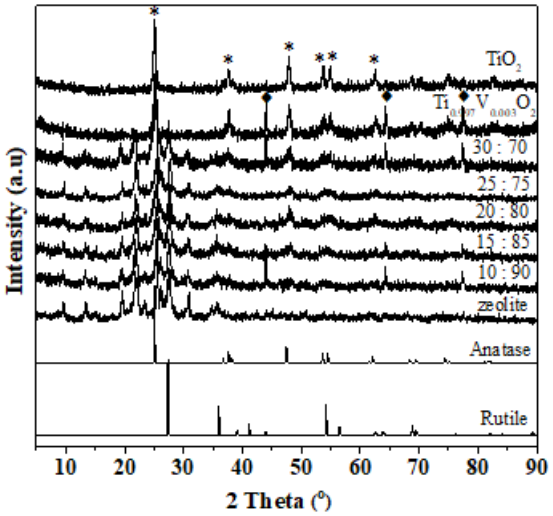

Figure 2. XRD pattern of mordenite zeolite, TiO_2, $Ti_{0.997}V_{0.003}O_2$, and $Ti_{0.997}V_{0.003}O_2$/zeolite at various composition.

It was previously reported that vanadium (0.3%) doped TiO_2 which is synthesized using sonochemical method does not induce the rutile phase at 500˚C [15]. So it can be concluded that the rutile formation induced by vanadium at little bit higher temperature (550˚C) in sonochemichal method. Since the insitu preparation was employed, there are any possibility for vanadium to interact not only with TiO_2 but also with Zeolite. XRD pattern for $Ti_{0.997}V_{0.003}O_2$/zeolite shown structural characteristic for both zeolite phase and $Ti_{0.997}V_{0.003}O_2$ i.e mordenite, anatase and rutil phase. The apparent of rutil phase in XRD spectra concluded that vanadium known to interact with TiO_2 lattice and does not undergo an ionic exchange interaction with zeolite.

Refinement for all XRD patterns of $Ti_{0.997}V_{0.003}O_2$/zeolite were employed with 3 standard of anatase, rutile and mordenite phase. Anatase phase crystallized in tetragonal lattice with $I4_1amd$ of space group and 4 of asymmetric unit (Z=4). Rutile phase shown tetragonal lattice with $P4_1/nmn$ of space group and 2 asymmetric unit (Z=2) while mordenite zeolite crystallized in orthorombic with $Ccmc$ of space group (Z=1). Mordenite found as the major phase compared with TiO_2 phase because of its dominant ratio in supported photocatalyst.

3.2. Spectroscopy Data

The IR spectra of all samples shown in Figure 3. Mordenite zeolite has observed peaks at ~ 466 cm^{-1}, 719 cm^{-1}, 794 cm^{-1}, 1062 cm^{-1}, shoulder at 1220, 1641 cm^{-1}, and boardband around 3459 cm^{-1}. Band at ~ 466 cm^{-1} attributed to bending vibration of T-O bond (T=Si, Al) in TO_4 tetrahedron [18-20]. Band at ~719 assigned to symmetrical stretching mode of O-T-O bond in internal tetrahedron while band at ~794 assigned to symmetric stretching in external linkage [20]. Band at ~1062 ascribed to O-T-O asymmetrical stretching in external linkage and band at ~1250 cm^{-1} due to O-T-O asymmetrical stretching mode in internal tetrahedron [20-21]. The band at 1641 cm^{-1} and 3459 cm^{-1} are associated with bending and stretching OH group of adsorbed water [21]. This bands also observed in IR spectra of TiO_2, $Ti_{0.997}V_{0.003}O_2$ and $Ti_{0.997}V_{0.003}O_2$/zeolite spectra. It can conclude that hydroxil group and adsorbed water are present on all photocatalyst. TiO_2 and $Ti_{0.997}V_{0.003}O_2$ shown peaks at 570-651 cm^{-1} which attributed to stretching vibration of Ti-O-Ti bond and the band at 1373-1383 cm^{-1} related to Ti-O-Ti structural network or lattice vibration [19]. The intensity of the band became weaker while vanadium introduced into the lattice indicating that vanadium successfully doped into TiO_2 lattice.

Figure 3 c shows that the membrane could remove PM2.5 particles (particulate matters with the size of less than 2.5 □m) almost completely (~99.9%). In addition, the membrane exhibited relatively low-pressure drops which are beneficial for their application. The lower pressure drop will result in lower energy consumption.

FTIR spectra for all $Ti_{0.997}V_{0.003}O_2$/zeolite photocatalyst having similar characteristic of parent structure. However, the bands have shifted due to interaction between photocatalyst and support material. The band at around 1062-1250 cm^{-1} experienced the highest deformation and shifting to higher wavenumber as $Ti_{0.997}V_{0.003}O_2$/zeolite ratio increased. It was indicated that immobilized $Ti_{0.997}V_{0.003}O_2$ on zeolite strongly influenced the asymmetrical vibration mode from internal and external linkage of mordenite zeolite. Strong deformation and shifting in internal and external linkage of zeolite indicating higher van der waals interaction between $Ti_{0.997}V_{0.003}O_2$ and zeolite which may affected by preparation method using ultrasonic irradiation. Transferred energy from ultrasound wave assisted $Ti_{0.997}V_{0.003}O_2$ to penetrate and well immobilized into mordenite zeolite resulted in strong van der waals interaction.

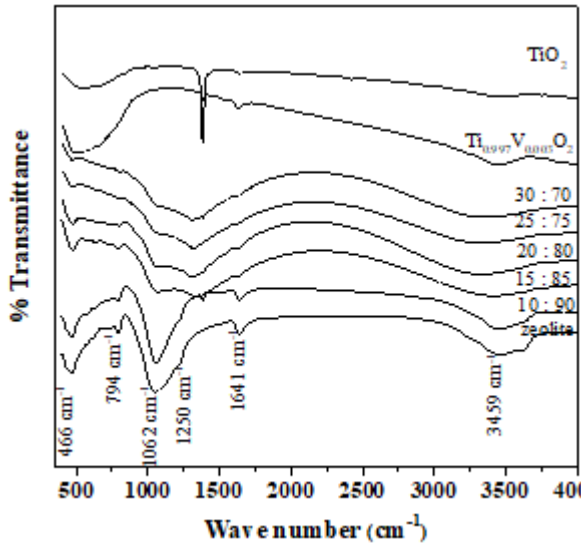

Figure 3. FTIR spectra of mordenite zeolite, TiO_2, $Ti_{0.997}V_{0.003}O_2$, and $Ti_{0.997}V_{0.003}O_2$/zeolite at various composition.

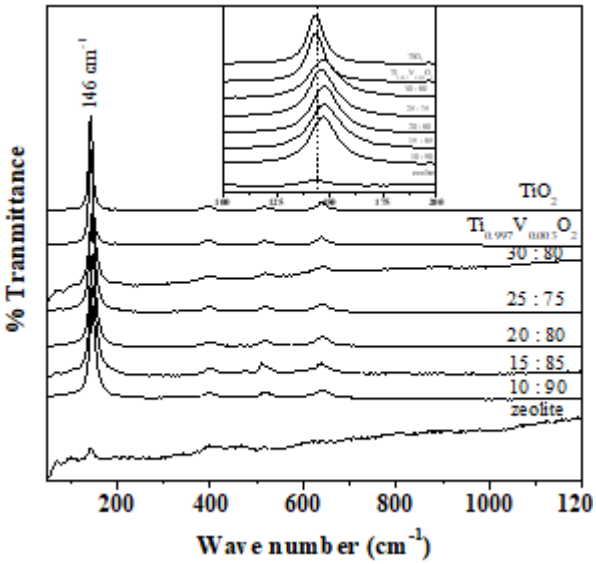

Figure 4. Raman spectra of mordenite zeolite, TiO_2, $Ti_{0.997}V_{0.003}O_2$, and $Ti_{0.997}V_{0.003}O_2$/zeolite at various composition.

Figure 4 shows raman spectra for mordenite zeolite, TiO_2, $Ti_{0.997}V_{0.003}O_2$, and $Ti_{0.997}V_{0.003}O_2$/zeolite. For mordenite zeolite found high fluorescence due to various elements contained in natural zeolite. It became difficult in obtaining appropriate signal to noise ratio from highly dispersed material. In the Raman spectra of TiO_2, $Ti_{0.997}V_{0.003}O_2$, and $Ti_{0.997}V_{0.003}O_2$/zeolite at any composition, similar local characteristic vibration were observed. All the vibration mode assigned to anatase vibration mode (Table 1).

However, no Raman peak at 233, 447, 611 cm^{-1} (RRUFF R110109) correspond to rutile phase which detected in XRD spectra. It may cause by low amount of rutile phase in sample and anatase phase shown predominantly. Further insight on the highest intensity at ~146 cm^{-1}, known that $Ti_{0.997}V_{0.003}O_2$/zeolite at any composition have shifted to higher wavenumber due to an interaction of supported $Ti_{0.997}V_{0.003}O_2$ and zeolite. It clearly shows that O-Ti-O bond in supported photocatalyst became tighten due to its van der waals force so that the vibration shifted to higher wavelength.

Table 1. The Assignment of vibration modes of Raman spectra

Peak Position (cm^{-1})	Vibration Mode	Assignment [22]
~146	E_g	Symmetric stretching vibration O-Ti-O
~199	E_g (weak)	Symmetric stretching vibration O-Ti-O
~399	B_{1g}	Symmetric bending vibration O-Ti-O
~516	A_{1g}	Asymmetric bending vibration O-Ti-O
~640	E_g	symmetric stretching vibration O-Ti-O

3.3. Optical Properties

DRS data in Figure 5 shows the reflectance properties of all samples. TiO_2 confirmed the high reflectance in visible wavelength. Unlike TiO_2, mordenite zeolite has no reflectance type of semiconductor material. Among all $Ti_{0.997}V_{0.003}O_2$/zeolite ratio, 15/85 w/w ratio resulted in the lowest reflectance at visible region 475-675 than another ratio. Transformation the reflectance data to Kubelka Munk function gave absorption coefficient over scattering properties F(R) as shown in Figure 6. Absorption properties at visible region revealed that 15:85 w/w ratio has higher absorption than the other photocatalyst while no significant differences obtained at ultraviolet region.

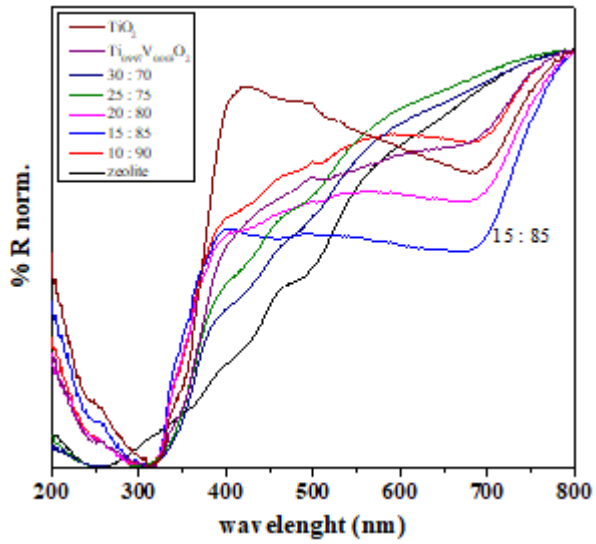

Figure 5. Reflectance spectra of mordenite zeolite, TiO_2, $Ti_{0.997}V_{0.003}O_2$, and $Ti_{0.997}V_{0.003}O_2$/zeolite at various composition.

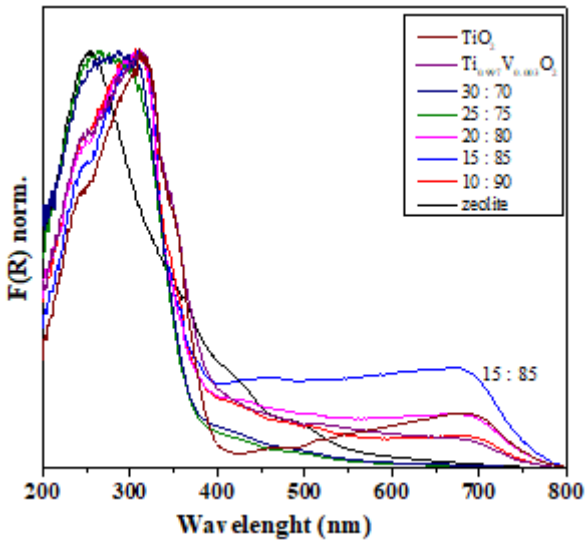

Figure 6. Kubelka-Munk function of mordenite zeolite, TiO_2, $Ti_{0.997}V_{0.003}O_2$, and $Ti_{0.997}V_{0.003}O_2$/zeolite at various composition.

Bandgap energy (E_g) of all samples were determined by plotting $(F(R)h\nu)^{½}$ versus photon energy ($h\nu$) as shown in Figure 7. Bandgap energy and absorption threshold for undoped TiO_2, $Ti_{0.997}V_{0.003}O_2$, and $Ti_{0.997}V_{0.003}O_2$/zeolite were listed in Table 2.

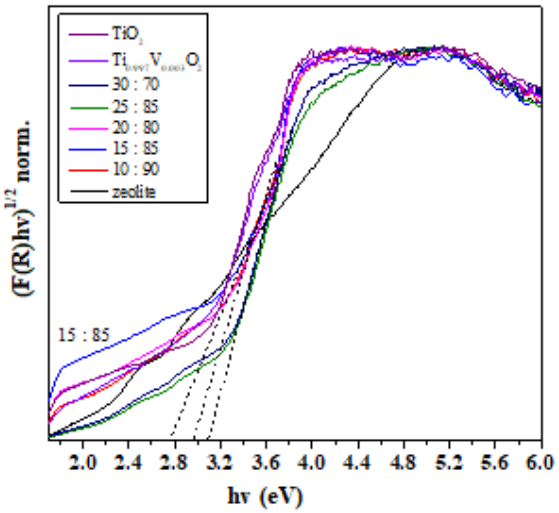

Figure 7. Bandgap energy of mordenite zeolite, TiO_2, $Ti_{0.997}V_{0.003}O_2$, and $Ti_{0.997}V_{0.003}O_2$/zeolite at various composition

Table 2. Bandgap Energy and Absorption edge of photocatalyst material

Sample	Band gap (eV)	Absorption threshold (nm)
TiO_2	2.9	427
$Ti_{0.997}V_{0.003}O_2$	2.8	443
10:90	2.9	427
15:85	2.77	447
20:80	2.85	435
25:75	3.15	393
30:70	3.13	396
Zeolite	-	-

Absorption threshold calculated by following relationship: $\lambda=1240/Eg$ Anatase TiO_2 is well known to have band gap energy about 3.2 eV which corresponding to absorption threshold 387 nm. Anatase phase of TiO_2 in this research had lower energy gap (2.9 eV) which is decreased to 2.8 eV while vanadium inserted into the lattice. Vanadium dopant clearly affected the band gap energy as predicted. However, the band gap energy of TiO_2 itself may affected by preparation method using ultrasonic irradiation. Further investigation on another characteristic such as particle size properties which may contribute to band gap properties. Supported photocatalyst regarding to research variable at various composition showed that 15/85 w/w ratio gained the lowest reduction in bandgap energy (2.77 eV, correspond to absorption edge 447 nm).

4. Conclusion

Supported photocatalyst of $Ti_{0.997}V_{0.003}O_2$/zeolite at 10/90, 15/85, 20/80, 25/75 and 30/70 % w/w ratio have been prepared using sonochemichal method. All $Ti_{0.997}V_{0.003}O_2$/zeolite samples have structural characteristic of anatase phase, rutil phase and mordenite zeolite. Vanadium known to induce rutile phase formation since no rutile phase detected in XRD pattern of TiO_2 itself with the same preparation method. Asymmetrical vibration mode in IR spectra at around 1062-1250 cm^{-1} which is related to internal and external linkage of modernite zeolite have been strongly deformed and shifted to higher wavenumber due to the increasing of van der waals interaction as $Ti_{0.997}V_{0.003}O_2$/zeolite ratio increased. Symmetrical stretching vibration of local structure also shifted to higher wavenumber caused by tightening bond between $Ti_{0.997}V_{0.003}O_2$ and zeolite. $Ti_{0.997}V_{0.003}O_2$/zeolite at 15/85 % w/w ratio produces the lowest reflectance and the highest absorption properties in visible light irradiation than the others composition. This ratio also achieved the lowest bandgap energy (2.77 eV).

Acknowledgement

The authors gratefully acknowledge to Religion Ministry of Republic of Indonesia for providing research funding, BOPTN (Bantuan Operasional Perguruan Tinggi Negeri) in LP2M UIN Maulana Malik Ibrahim.

References

[1] Padmini E and Miranda L R 2013 Chem. Eng. J 232 249-258
[2] Shao G N, Jeon S J, Haider M S, Abbas N and Kim H T 2016 J. Colloid Interface Sci 474 179-189
[3] Choi J, Park H, and Hoffman M R 2009 J. Mater. Res 25 149-158
[4] Kahatta C, Wongpisutpaisan N, Vittayakorn N, and Pecharapa W 2013 Ceram. Int. 39 S389-S393
[5] Khatun N, Rini E G, Shirage P, Rajput P, Jha S N and Sen S 2016 Mater. Sci. Semicond. Process 50 7-13
[6] Nyamukamba, P., Tichagwa, L., & Greyling, C. 2012 Mater. Sci. Forum 712 49–63
[7] Xie, W., Li, R., & Xu, Q. 2018 Scientific Reports 1–10.
[8] Meksi, M., Hamandi, M., Berhault, G., Guillard, C., & Kochkar, H. 2015 Chem. Lett. 44(12) 1774
[9] Juan C. C., Magdziarz A., Kuszydlowdski K., Gronzka J., Chernyeyeva O., and Lisovytskiya D 2013 Appl. Catal., B 134-135 136-144
[10] Guesh K., Alvarez C.M., Chebude Y. and Diaz I. 2016 Appl. Surf. Sci. 378 473-478
[11] Fangfei Li, Jiang Y, Yu L., Yang Z., Hou T. and Sun S. 2005 Appl. Surf. Sci. 252 1410-1416
[12] Okte A N, and Yilmaz O 2009 Microporous Mesoporous mater. 126 245-252
[13] Alwash A H, Abdullah A Z, and Ismail N 2012 J. Hazard. Mater. 233-234 184–193
[14] Huang M, Xu C, Wu Z, Huang Y, Lin J, and Wu J 2008 Dyes Pigm. 77 324-334
[15] N Aini et al 2018 IOP Conf. Ser.: Mater. Sci. Eng. 333 012020
[16] Mukti, R. R., Wustoni, S., Wahyudi, A., & Ismunandar. 2013 Indonesian Journal of Chemistry 13(3) 278–282
[17] Bang J H and Suslick K S 2010 Adv.Mater 22 1039-1059
[18] Byrappa K and Kumar B.V.S 2007 Asian Journal of Chemistry 19(6) 4933-4935
[19] Chen K, Li J, Wang W, Zhang Y, Wang X, and Su H 2011 Applied Surface Science 257 7276-7285
[20] Auerbach, M. (n.d.). Zeolite Science and Technology. Marcel Dekker. New York. ISBN: 0-8247-4020-3
[21] Binitha N N, Sugunan S, 2006 Macroporous Mesoporous Mater 93 82-89
[22] Ramasamy, P., Lin, D.H., Kim, J., and Kim, J. 2013 RSC Adv. 4(6) 2858-2864